

Atomic ordering-induced band gap reductions in GaAsSb epilayers grown by molecular beam epitaxy

B. P. Gorman^{a)}

Department of Materials Science and Engineering, University of North Texas, Denton, Texas 76203

A. G. Norman

National Renewable Energy Laboratory, Golden, Colorado 80401

R. Lukic-Zrnica and C. L. Littler

Department of Physics, University of North Texas, Denton, Texas 76203

H. R. Moutinho

National Renewable Energy Laboratory, Golden, Colorado 80401

T. D. Golding

Department of Physics, University of North Texas, Denton, Texas 76203

A. G. Birdwell

MEMC Electronic Materials, Inc., Sherman, Texas 75090

(Received 4 August 2004; accepted 22 October 2004; published online 1 March 2005)

A series of GaAs_{1-x}Sb_x epilayers ($0.51 < x < 0.71$) grown by molecular-beam epitaxy on GaAs substrates with surface orientations of (001), (001) -8° toward (111)A, (001) -8° toward (111)B, (115)A, (115)B, (113)A, and (113)B were investigated using temperature-dependent Fourier transform infrared (FTIR) spectroscopy and transmission electron microscopy. Atomic ordering in these epilayers was observed from a decrease in the energy gap measured by FTIR absorption and corroborated by superlattice reflections in electron diffraction. Contrary to previous investigations of ordering in III-V alloys, a marked energy-gap reduction, corresponding to CuPt-B-type ordering, is observed in the GaAs_{1-x}Sb_x grown on (111)A-type substrate offcuts. © 2005 American Institute of Physics. [DOI: 10.1063/1.1834983]

INTRODUCTION

GaAs_{1-x}Sb_x is a promising material for the fabrication of electronic and optoelectronic devices, with technological potential that has been studied in conjunction with other III-V alloys for various applications such as heterojunction bipolar transistors,¹ double heterostructure lasers,² and vertical cavity surface emitting lasers.³ In addition, GaAs_{1-x}Sb_x exhibits strong atomic ordering when grown by molecular-beam epitaxy (MBE).⁴⁻⁸ Spontaneous ordering causes changes in the electronic properties and, as such, it can be useful in the engineering of optoelectronic devices where energy-gap tailoring is needed.⁹

Ordering has been observed in many III-V semiconductor alloy systems, including Al_xIn_{1-x}As, In_xGa_{1-x}As, and In_xGa_{1-x}P.^{10,11} Different designations for the types of ordering (i.e., CuPt-A, CuPt-B, and CuAu) are used, depending upon the crystallographic direction of the ordered atomic planes. The most investigated type of ordering, CuPt-B, is formed along only the two $\langle 111 \rangle$ B-type directions. It has been suggested^{12,13} that this is a result of the reconstruction of the growing surface and that incorporation of atoms at surface steps plays a critical role in the ordering process. A fundamental understanding of the origins of these types of ordering is still needed in order to utilize the ordered materials in engineered devices successfully.

In this paper, we present energy-gap reduction data and ordering parameter estimations obtained from Fourier transform infrared (FTIR) absorption spectroscopy studies of GaAs_{1-x}Sb_x epilayers grown on different orientations of GaAs in order to elucidate the role of substrate orientation on spontaneous atomic ordering. Absorption results will be compared to the observed superlattice spot intensities in transmission electron diffraction (TED) patterns to qualitatively relate the observed ordering-induced band-gap reduction.

EXPERIMENT

GaAs_{1-x}Sb_x epilayers ($0.51 < x < 0.71$) were grown using MBE on GaAs substrates with surface orientations of (001), (001) -8° toward (111)A, (001) -8° toward (111)B, (115)A, (115)B, (113)A and (113)B. The series of substrate orientations was chosen to induce a range of order parameters. A VG V80H MBE system used at the Blakett Laboratory, Imperial College, utilized As₄, Sb₄, and Ga as sources. Alloy compositions were controlled using Ga and Sb incorporation rates determined using reflection high-energy electron diffraction (RHEED) intensity oscillations. GaAs buffer layers were initially grown on the cleaned substrate at 580 °C. Film growth rates were kept constant at approximately 1 μm/h, and the substrate temperature held at 525 °C. Film growth parameters, compositions, and substrate orientations are summarized in Table I.

^{a)}Electronic mail: bgorman@unt.edu

TABLE I. GaAs_{1-x}Sb_x film growth properties and ordering parameters calculated from the band-gap decrease relative to that predicted from its composition.

Sample	Substrate orientation	Sb content (<i>x</i>) from XRD and (EPMA)	Growth temp (°C)	E_g calculated (eV)	E_g measured (eV)	<i>S</i>
472	(115) <i>B</i>	0.529 (0.514)	525	0.761	0.713	0.27
473	(001)	0.647	525	0.703	0.658	0.27
474	(115) <i>A</i>	0.643 (0.618)	525	0.704	0.550	0.49
478	(001) 8° → (111) <i>B</i>	0.568	525	0.738	0.692	0.27
479	(001)	0.669 (0.669)	525	0.696	0.650	0.27
480	(001) 8° → (111) <i>A</i>	0.650	525	0.702	0.642	0.31
483	(113) <i>A</i>	0.711 (0.654)	525	0.686	0.629	0.30
484	(001)	0.688	525	0.691	0.672	0.17
485	(113) <i>B</i>	0.511 (0.496)	525	0.772	0.745	0.21

Following the growth of GaAs_{1-x}Sb_x epilayers approximately 2 μm thick, compositions were determined using double-crystal x-ray diffraction (XRD). For the samples grown on ⟨001⟩-oriented substrates, XRD measurements were made both of the (004) and the asymmetric (115) reflections that enabled the degree of relaxation of the samples to be measured and the alloy composition to be determined accurately. The results were also corrected for layer tilt by taking measurements with the sample rotated at 0° and 180°. The ⟨001⟩ layers were found to be between 90% and 95% strain relaxed. Using these same techniques, accurate compositions were also determined for the (001) 8° toward (111) offcut samples.

For the samples grown on (115)- and (113)-oriented substrates, the XRD measurements were made with (115) and (113) reflections, respectively, and the alloy compositions calculated assuming the layers were 100% relaxed. However, due to the different relaxation mechanisms expected for these non-(001) substrate orientations it is expected that the degree of strain relaxation in these samples may be considerably lower than those measured for the (001) substrate samples. In order to double check the accuracy of the compositions deduced from the XRD measurements for these offcut samples, wavelength dispersive x-ray electron microprobe analysis (EPMA) measurements were performed using a (001)-oriented substrate GaAs_{1-x}Sb_x sample of known composition as a compositional standard. Comparisons of the compositions determined using XRD and EPMA (Table I) illustrate that the EPMA-measured Sb contents of the *B* offcut layers are slightly less, but the *A* offcuts are quite a bit lower than the XRD-measured Sb contents. The implications of these compositional discrepancies on the ordering parameters will be discussed later.

The optical properties of the GaAs_{1-x}Sb_x epilayers were investigated using temperature-dependent FTIR spectroscopy. Samples were mounted in a variable-temperature cryostat and aligned with the film surface normal to the infrared beam. Transmission spectra were acquired using a mercury cadmium telluride (MCT) detector over the range of 0.2–1.4 eV. Film thickness and refractive indexes were determined using a technique described previously¹⁴ over the temperature range of 4–300 K. As seen in Fig. 1, the energy gap, E_g , at each temperature was determined assuming a parabolic

band structure¹⁵ from the extrapolation of the slope of the absorption coefficient squared versus the photon energy to the zero value base line.

Since FTIR absorption spectroscopy cannot directly measure the ordering parameter (*S*), only qualitative measurements of *S* can be made. In order to estimate the degree of ordering from the observed energy-gap reduction, the theoretical approach proposed by Zunger and Mahajan¹⁶ and Wei *et al.*¹⁷ was employed. They proposed the following expression to describe the energy-gap reduction, resulting from the presence of CuPt-*B*-type ordering in an alloy system

$$\Delta E_g(S) = E_g(S) - E_g(0) = \Delta E_g(1) \cdot S^2, \quad (1)$$

where $\Delta E_g(S)$ is the value of the reduced energy gap obtained from the calculated differences for the random alloy [$E_g(0)$] and the values obtained from the absorption measurements [$E_g(S)$]. The variation of the energy gap, $E_g(0)$, with composition for the random GaAs_{1-x}Sb_x alloy predicted by Nahory *et al.*¹⁸ is given by $E_g = 1.43 - 1.9x + 1.2x^2$. This formula was obtained from the results of photoluminescence measurements of the random GaAs_{1-x}Sb_x alloys grown by liquid phase epitaxy of varying *x* value at room temperature. This expression agrees well with the experimental results obtained by different optical techniques.^{5,18–20} The energy-

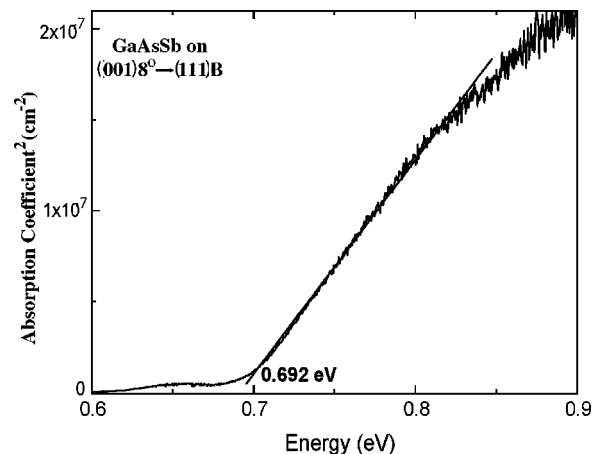


FIG. 1. Absorption coefficient squared vs photon energy for a GaAs_{0.432}Sb_{0.568} epilayer on a (001)–8° toward (111)*B* GaAs measured at 300 K. The extrapolation of the data gives a band-gap value of 0.692 eV at 300 K.

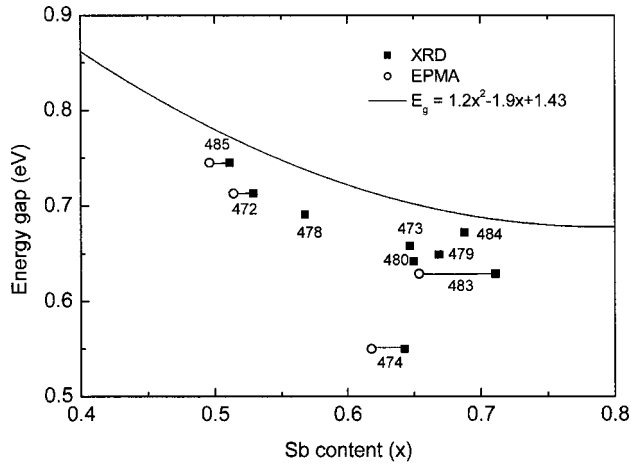


FIG. 2. Room-temperature energy gap vs composition for a series of $\text{GaAs}_{1-x}\text{Sb}_x$ epilayers. The results of this work are shown as solid squares. All samples exhibit some degree of CuPt- B -type ordering.

gap reduction, $\Delta E_g(1)$, for fully ordered systems has been theoretically calculated for most III-V ordered alloys.^{9,16,17} The calculated $\Delta E_g(1)$ for $\text{GaAs}_{1-x}\text{Sb}_x$ was determined using the method described by Zunger and Mahajan.¹⁶ The difference between the corrected random-alloy energy gap calculated from the SQS-4 model and the calculated fully ordered energy gap was used as $\Delta E_g(1)$. Equation (1) was then utilized to deduce S from the measured $E_g(S)$.

Transmission electron microscopy (TEM) and diffraction (TED) were also employed to observe the ordering effects in the epilayers. Cross-sectional and plan-view samples were prepared using standard techniques and examined in a Philips CM30 TEM at 300 kV. The strength and arrangement of TED superlattice spots were assessed in order to determine qualitatively the amount and type of the ordering. Dark field and high-resolution TEM images were employed to further investigate the microstructure of the layers.

RESULTS

The energy gaps (E_g) of the MBE-grown layers were obtained from the temperature-dependent FTIR transmission measurements, as illustrated previously.¹⁴ As shown in Fig. 2, the observed room-temperature energy gaps were found to be less (by varying degrees) than those predicted by the standard energy gap versus the composition expression for a random alloy.¹⁸⁻²⁰ As seen in Table I, the differences between the predicted and measured values for the presently investigated samples lie between 10 and 150 meV. As mentioned earlier, slight discrepancies in the film compositions were obtained from the XRD and EPMA measurements. From Table I and Fig. 2, it can be seen that a range of $E_g(S)$ values can be obtained from the XRD and EPMA composition values. Due to the higher Sb content, and thus smaller energy-gap reductions, values of S were calculated using the XRD compositional data.

The reduction of energy gap has been noted before at room temperature in MBE-grown GaAsSb layers^{19,21} but never to such an extent. In order to confirm that the reduction in energy gap is due to CuPt-type ordering, TED measurements were performed on a representative set of samples.

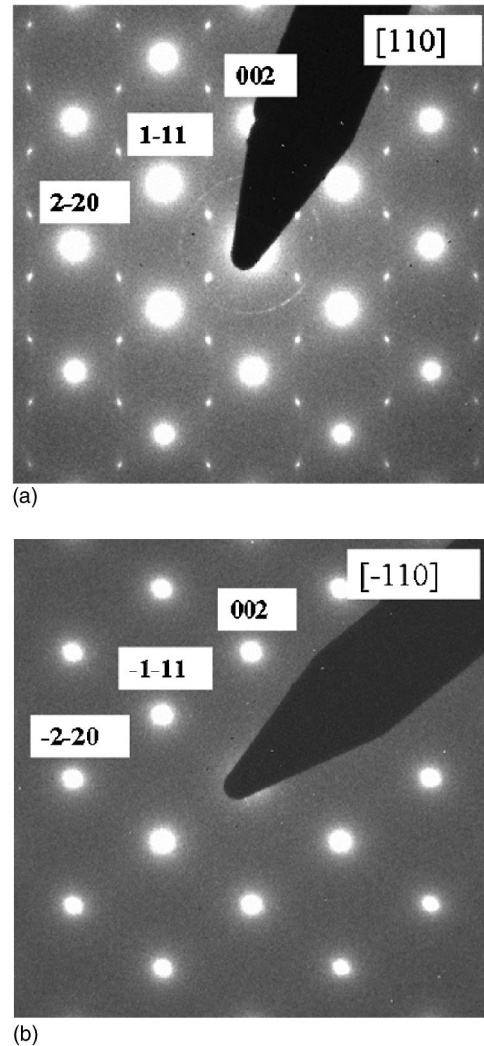


FIG. 3. Selected area transmission electron-diffraction pattern of sample 483 grown on (113)A GaAs, illustrating a strong degree of ordering on both sets of $\{111\}B$ planes. (a) $[110]$ zone and (b) $[\bar{1}10]$ zone.

The TED measurements illustrate that samples grown on the (113)A and (115)A orientation GaAs substrates contained domains of a rather strong CuPt ordering on both sets of $\{111\}B$ planes. Figures 3 and 4 show the $[110]$ and $[\bar{1}10]$ zone TED patterns for samples 483 ($x=0.711$) and 474 ($x=0.643$). In the $[\bar{1}10]$ TED pattern, only diffraction spots due to the zinc-blende structure are observed. However, in the $[110]$ pattern, strong superlattice reflections corresponding to the ordered structure at $\pm 1/2[\bar{1}11]$ and $\pm 1/2[1\bar{1}1]$ from each fundamental reflection are present. The presence of these half-ordered diffraction spots in the TED patterns implies that ordering on the $(\bar{1}11)$ and $(1\bar{1}1)$ planes has occurred. The relative strength of the superlattice spots was lower in the sample grown on (113)A than in the sample grown on (115)A. This result correlates well with the absorption measurements, which indicated energy-gap reductions of ≈ 50 meV and ≈ 150 meV, respectively, for these two samples.

Figure 5 shows diffraction patterns obtained from two orthogonal $\langle 110 \rangle$ cross sections of sample 472 ($x=0.529$) grown on (115)B GaAs. Diffraction patterns at the $[\bar{1}10]$

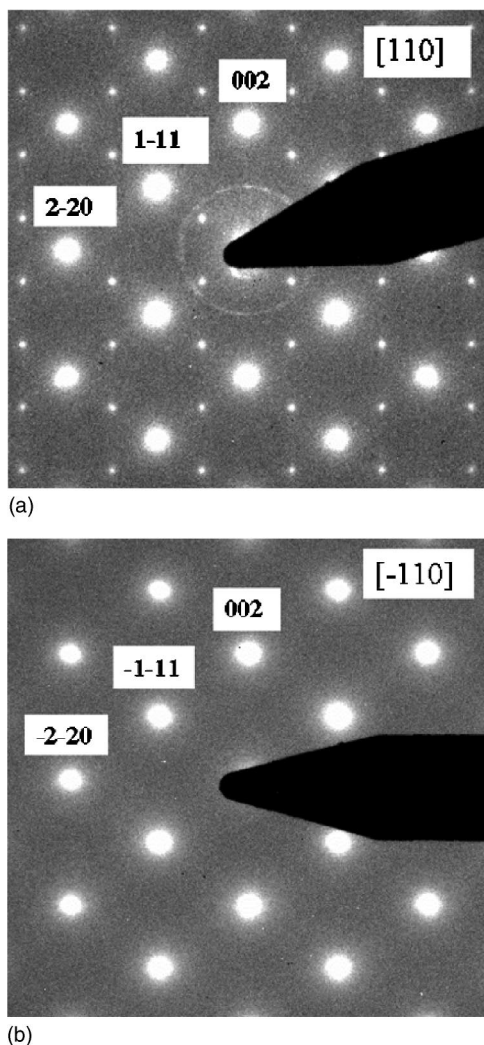


FIG. 4. Selected area transmission electron-diffraction pattern of sample 474 grown on (115)A GaAs, illustrating a very strong degree of ordering on both sets of $\{111\}B$ planes. (a) $[110]$ zone and (b) $[\bar{1}10]$ zone.

zone axis only exhibit the Bragg reflections of the fundamental zinc-blende structure. In the $[110]$ zone axis pattern, (111) superlattice spots of medium strength are present in addition to the base matrix spots, indicating the doubling in periodicity of the crystal structure along the $[\bar{1}11]$ direction. These results demonstrate the formation of the $[111]$ variant of the CuPt-type ordered structure in the $\text{GaAs}_{1-x}\text{Sb}_x$ layer grown on (115)B GaAs. This sample showed an energy-gap reduction of ≈ 50 meV in comparison to that predicted for a random alloy of the same composition correlating well with the relative strength of superlattice spots observed for this sample. In Fig. 6, a Fourier filtered lattice image of sample 472, ordered domains corresponding to the single variant of the CuPt-B-type ordering observed in this sample are visible.

Figure 7 shows the diffraction patterns from sample 479 ($x=0.669$) grown on (001) GaAs. The diffraction spots in Fig. 7 indicate weak ordering on both sets of $\{111\}B$ planes in the examined cross section. According to previous studies on these alloy materials,^{6,22} it was expected that the (001) substrate orientation would provide a larger degree of ordering than was observed for this particular sample.

In addition to atomic ordering, other factors may also

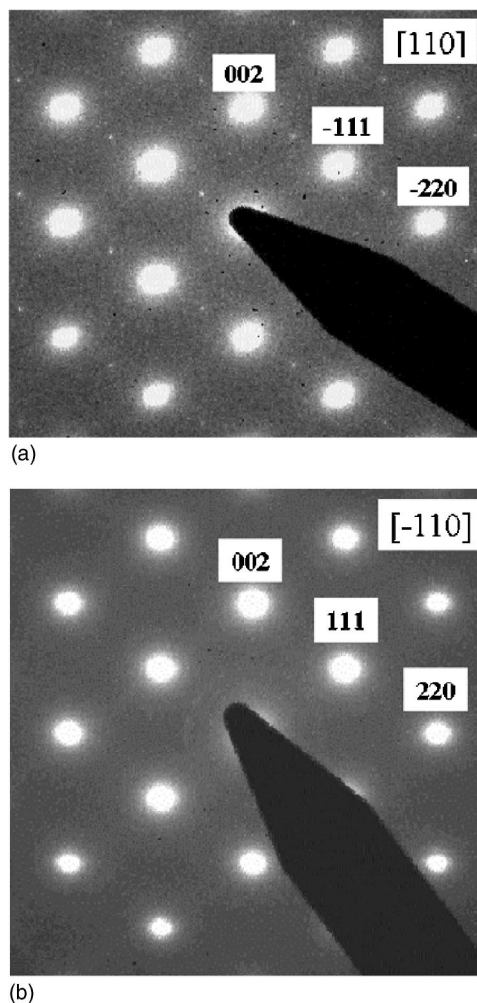


FIG. 5. Selected area transmission electron-diffraction pattern of sample 472 grown on (115)B GaAs, illustrating a medium degree of ordering on only the $(111)B$ planes. (a) $[110]$ zone and (b) $[\bar{1}10]$ zone.

contribute to the band-gap reduction. In particular, phase separation in samples with $x < 0.7$ may cause a band-gap reduction if a second, Sb-rich, phase was present (see Nakhory compositional dependence of the band gap in Fig. 2).

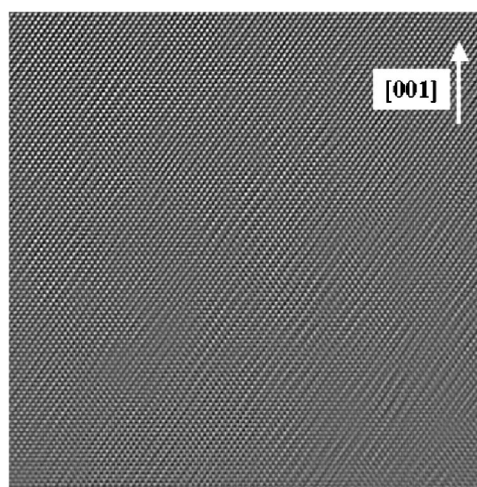


FIG. 6. Fourier filtered lattice image of $[110]$ cross section, showing atomic ordering on only the $(111)B$ planes for sample 472 grown on (115)B GaAs.

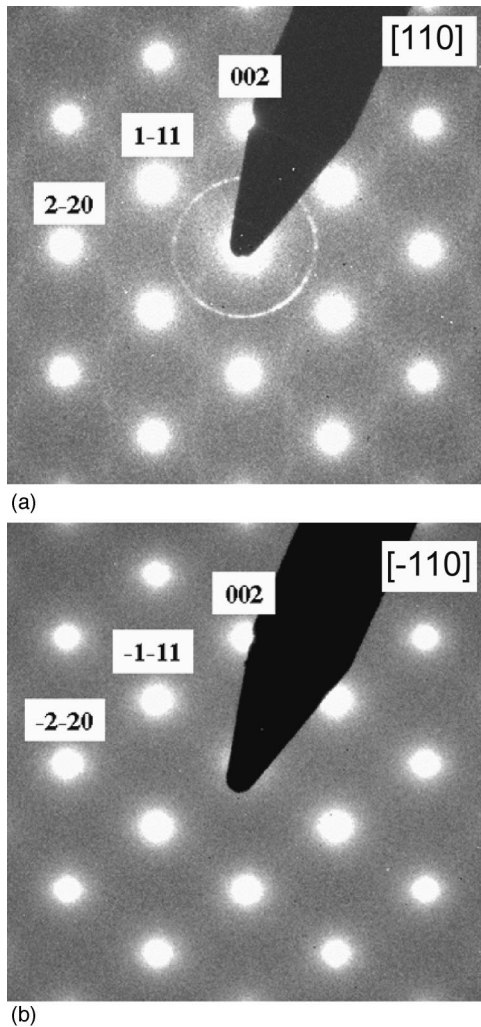


FIG. 7. Selected area transmission electron-diffraction pattern of sample 479 grown on [001] GaAs, illustrating the lowest degree of ordering on both sets of $\{111\}B$ planes. (a) $[110]$ zone and (b) $[\bar{1}\bar{1}0]$ zone.

Previous studies of low-temperature grown MBE $\text{GaAs}_{1-x}\text{Sb}_x$ alloys have revealed phase separation by the splitting of primary diffraction spots as well as by the structure factor contrast in dark field TEM.¹¹ As seen in Figs. 3–5 and 7, no splitting of the primary diffraction spots is present, indicating the lack of phase separation in the $\text{GaAs}_{1-x}\text{Sb}_x$ alloys. Figure 8 is a chemically sensitive (002) reflection dark field image of sample 474, which has the largest band-gap reduction in this study. The lack of contrast in this image, apart from that due to the threading defects in the layer, indicates an absence of phase separation in the alloy, and further indicates that the band-gap reduction is due to the atomic ordering and not to the phase separation.

From these results it can be concluded that the observed energy-gap reduction for the $\text{GaAs}_{1-x}\text{Sb}_x$ layers is indeed caused by the formation of the ordered structure. It should be noted that the energy-gap value for a $\text{GaAs}_{1-x}\text{Sb}_x$ alloy at a given composition of $x=0.643$ is 0.55 eV. Such a large energy-gap reduction was due to the CuPt-*B*-type atomic ordering in this III-V-V-type alloy.

Upon comparing the calculated order parameter (S) with the TED results for samples 474 and 472 (Fig. 4 and 5), the

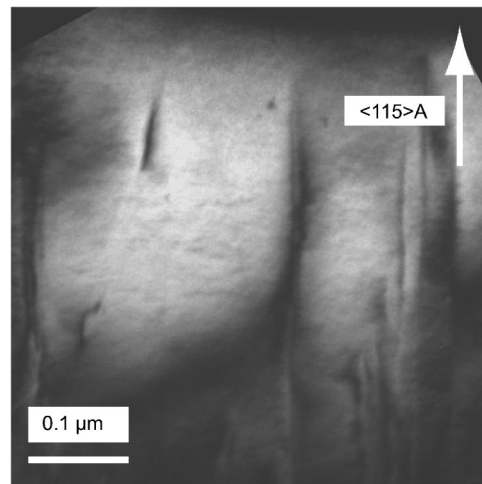


FIG. 8. Chemically sensitive (002) reflection dark field TEM image of sample 474, illustrating no phase separation present in the GaAsSb layer.

relative degree of ordering visible in the intensities of the superlattice reflections qualitatively correlate well with the magnitude of the energy-gap reductions. The value of S is somewhat larger than that expected and may be attributed to either the errors in the calculation of the random-alloy composition band gap, the theoretically determined band gap for the fully ordered alloy, or the limitations of the theoretical method used to calculate the ordering parameter. Due to the applicability of the random-alloy calculation to other $\text{GaAs}_{1-x}\text{Sb}_x$ studies, the main overestimation likely lies with either the ordering parameter calculation or the fully ordered alloy band-gap calculation. As seen in a previous work,²³ the S^2 dependence on the band-gap reduction does not agree with the experimental data obtained for GaInP, and this may also be the case for other III-V alloys. Although the value of the energy-gap reduction for the completely ordered alloy is believed to be overestimated and is only applicable at $x=0.5$, it is the only theoretically calculated value found in the literature for the $\text{GaAs}_{1-x}\text{Sb}_x$ alloy.

From Table I and the TED results, it is evident that the samples grown on the (111)*A*-type offcuts (i.e., samples 474, 480, and 483) exhibited a higher degree of ordering than the samples grown on (111)*B*-type offcuts and (001) substrate orientations. This is the opposite behavior to that exhibited by GaInP layers grown by metal organic vapor phase epitaxy where layers grown on (111)*A*-type offcuts were found to be much less ordered than the layers grown on (001)- and (111)*B*-type offcut substrates.²⁴ In fact, among the samples investigated, the three samples having the largest energy-gap reductions were all grown on the (111)*A*-type offcuts. This suggests that *A*-type steps play an important role in the CuPt-*B*-type ordering process in MBE $\text{GaAs}_{1-x}\text{Sb}_x$ layers.

The observation of the strongest atomic ordering in the (111)*A*-type offcut substrate samples could also arise if significant roughening of the growth surfaces occurred locally, producing a large surface area having orientations close to exact (001) and/or offcut a few degrees towards the (111)*A* or (111)*B* direction that could generate CuPt-*B*-type ordering (e.g., see Chap. 1 Sec. 2.4 of Ref. 10). This was checked by performing atomic force microscopy (AFM) on the surfaces

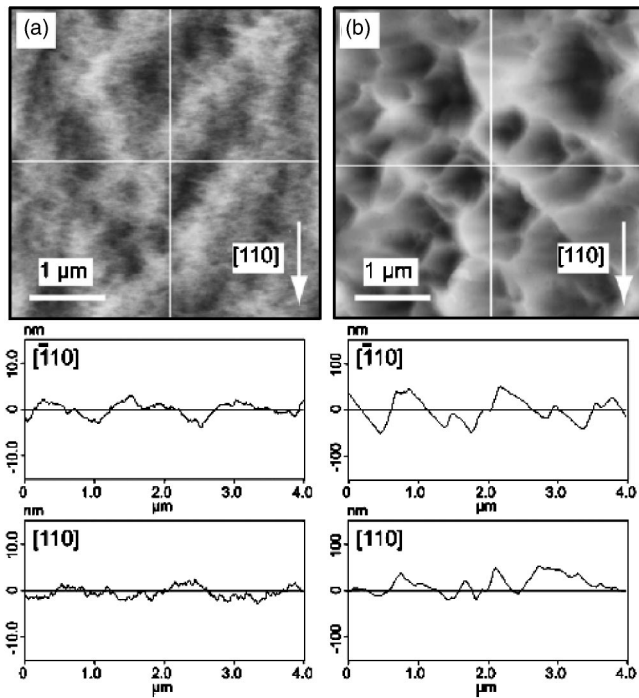


FIG. 9. AFM images and AFM line profiles in the $[110]$ and $\bar{[110]}$ directions of the surface of the following GaAsSb samples: (a) (115)A (sample 474), (b) (115)B (sample 472). The image height scale is 30 nm for (a) and 300 nm for (b). Note the much flatter surface of the (115)A sample.

of the majority of the samples. The results are illustrated in Fig. 9–11 which show AFM images and AFM line profiles along the $[110]$ and $\bar{[110]}$ directions of the surfaces of the samples grown on (115)A-, (115)B-, (113)A-, (113)B-, and (001)-oriented substrates, respectively. In addition, the root-

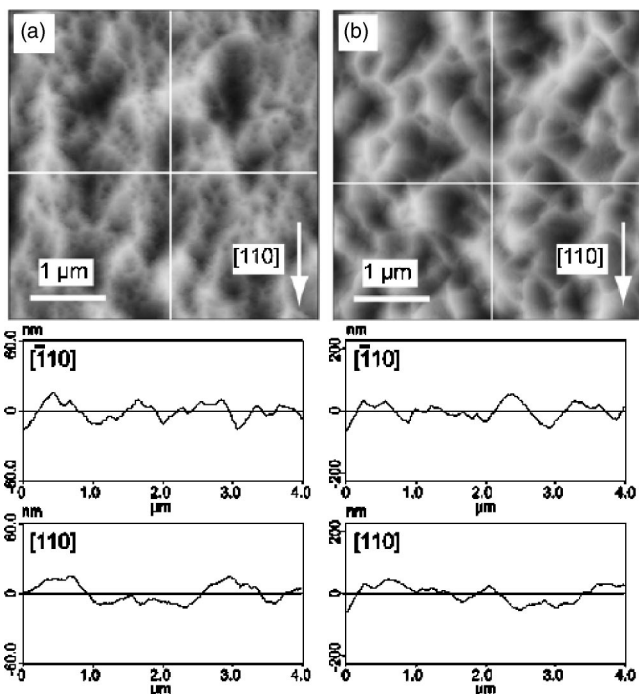


FIG. 10. AFM images and AFM line profiles in the $[110]$ and $\bar{[110]}$ directions of the surface of the following GaAsSb samples: (a) (113)A (sample 483), (b) (113)B (sample 485). The image height scale is 120 nm for (a) and 450 nm for (b). Note the much flatter surface of the (113)A sample.

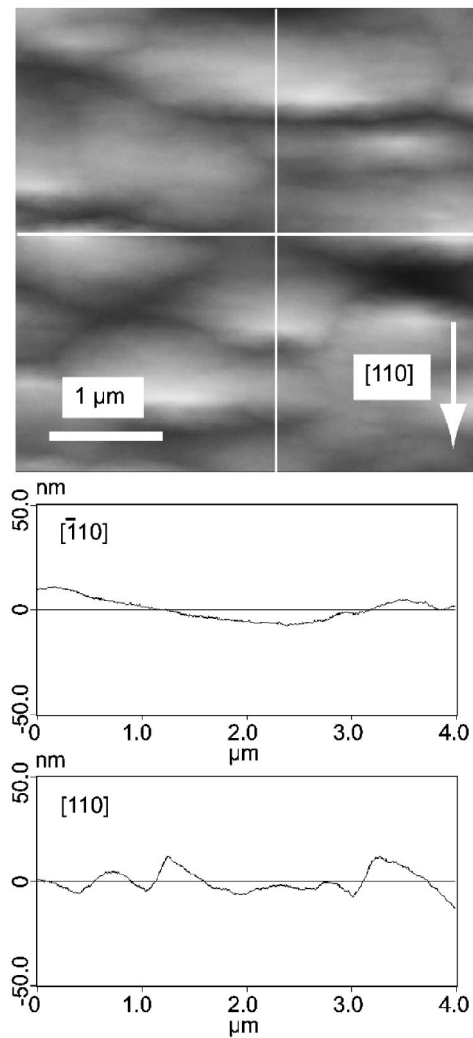


FIG. 11. AFM image and AFM line profiles in the $[110]$ and $\bar{[110]}$ directions of the surface of (001) GaAsSb (sample 484). The height scale of the image is 100 nm.

mean-square (rms) roughness values were determined from $4\ \mu\text{m} \times 4\ \mu\text{m}$ scan areas and are listed in Table II. From Fig. 9–11 and Table II it can be seen that the (111)A-type offcut surfaces are much flatter than the (111)B-type surface offcuts. In fact, the rms roughness values of the (115)A and (113)A samples are comparable to that measured for the (001) surface samples. If one compares the AFM line profiles for the highest-ordered sample [474, grown on (115)A, Fig.

TABLE II. GaAs_{1-x}Sb_x film surface roughness as determined by atomic force microscopy (AFM).

Sample	Substrate orientation	Sb content (x) from XRD		Roughness (nm)
		and (EPMA)		
472	(115)B	0.529	(0.514)	22.7
474	(115)A	0.643	(0.618)	1.6
478	(001) $8^\circ \rightarrow (111)B$	0.568		9.9
479	(001)	0.669 (0.669)		2.2
480	(001) $8^\circ \rightarrow (111)A$	0.650		2.9
483	(113)A	0.711 (0.654)		6.5
484	(001)	0.688		5.0
485	(113)B	0.511 (0.496)		26.8

9(a)] with the line profiles of the weakly ordered (001) sample (484, Fig. 11), it can be seen that the surface of the (115)*A* sample has much less surface area with local misorientations of exact (001) or offcut a few degrees from (001) towards the (111)*A* and/or (111)*B* direction. The highly ordered (115)*A* sample 474 also has much less surface area with these local misorientations than the less-ordered (111)*A* and (111)*B* offcut samples or exact (001) surface. These AFM results therefore strongly suggest that *A*-type steps do indeed play an important role in the CuPt-*B*-type ordering process in MBE GaAs_{1-x}Sb_x layers.

Also of note is the fact that these samples have slightly smaller dependences of E_g with temperature.¹⁴ This suggests the parameters that define the temperature shift of E_g (thermal and electron phonon coupling effects) may be dependent on the degree of ordering. One of the reasons for this behavior might be the modification in lattice dilatation due to the change of crystal symmetry, which is the consequence of the presence of atomic ordering, as seen in other work.²⁵ Raman spectroscopy studies are currently underway in order to evaluate the phonon-ordering relationship in these materials.

CONCLUSIONS

Atomic ordering in GaAs_{1-x}Sb_x epilayers grown by MBE on GaAs substrates was observed from a decrease in the energy gap measured by FTIR absorption and corroborated by the presence of superlattice reflections in electron diffraction. A significant energy-gap reduction, corresponding to CuPt-*B*-type ordering, was observed in the GaAs_{1-x}Sb_x grown on (111)*A*-type substrate offcuts, which is contrary to the studies of ordering in other III-V alloys in which (111)*B*-type offcuts produce the largest degree of ordering.

ACKNOWLEDGMENTS

The authors would like to thank Dr. Linda Hart for x-ray diffraction measurements and Bobby To for electron microprobe microanalysis measurements. This work is supported in part by the State of Texas Advanced Research Program

Project No. 003652-0472b-1999, the U.S. Army Office, the U.S. Department of Energy Basic Energy Sciences program, and the UK EPSRC.

- ¹S. P. Watkins, O. J. Pitts, C. Dale, X. G. Xu, M. W. Dvorak, N. Matine, and C. R. Bolognesi, *J. Cryst. Growth* **221**, 59 (2000).
- ²R. E. Nahory and M. A. Pollack, *Appl. Phys. Lett.* **27**, 562 (1975).
- ³J. Jaros, I. Ecker, and K. J. Ebeling, in *Proceedings of CLEO/Europe*, Nice, France, August 2000 (unpublished).
- ⁴I. J. Murgatroyd, A. G. Norman, G. R. Booker, and T. M. Kerr, *Proceedings of the 11th International Conference on Electron Microscopy*, Kyoto, Japan, 1986 [*J. Electron Microsc.* **35**, 1497 (1986)].
- ⁵Y. E. Ihm, N. Otsuka, J. Klem, and H. Morkoc, *Appl. Phys. Lett.* **51**, 2013 (1987).
- ⁶I. J. Murgatroyd, A. G. Norman, and G. R. Booker, *J. Appl. Phys.* **67**, 2310 (1990).
- ⁷Z. Zhong, *et al.* *Phys. Rev. B* **63**, 033314 (2001).
- ⁸I. G. Batyrev, A. G. Norman, S. B. Zhang, and S.-H. Wei, *Phys. Rev. Lett.* **90**, 026102 (2003).
- ⁹S.-H. Wei and A. Zunger, *Appl. Phys. Lett.* **56**, 662 (1990).
- ¹⁰*Spontaneous Ordering in Semiconductor Alloys*, edited by A. Mascarenhas (Kluwer, Dordrecht, 2002).
- ¹¹A. G. Norman, T.-Y. Seong, I. T. Ferguson, G. R. Booker, and B. A. Joyce, *Semicond. Sci. Technol.* **8**, S9(1993).
- ¹²B. A. Phillips, A. G. Norman, T. Y. Seong, S. Mahajan, G. R. Booker, M. Skowronski, J. P. Harbison, and V. G. Keramidas, *J. Cryst. Growth* **140**, 249 (1994).
- ¹³S. B. Zhang, S. Froyen, and A. Zunger, *Appl. Phys. Lett.* **67**, 3141 (1995).
- ¹⁴R. Lukic-Zrnica, B. P. Gorman, R. J. Cottier, T. D. Golding, C. L. Littler, and A. G. Norman, *J. Appl. Phys.* **92**, 6939 (2002).
- ¹⁵J. I. Pankove, *Optical Processes in Semiconductors* (Dover, New York, 1971).
- ¹⁶A. Zunger and S. Mahajan, *Handbook on Semiconductors*, edited by T. S. Moss (Elsevier, Amsterdam, 1994), p. 1399.
- ¹⁷S.-H. Wei, D. B. Laks, and A. Zunger, *Appl. Phys. Lett.* **62**, 1937 (1993).
- ¹⁸R. E. Nahory, M. A. Pollack, J. C. DeWinter, and K. M. Williams, *J. Appl. Phys.* **48**, 1607 (1977).
- ¹⁹J. Klem, D. Huang, H. Morkoc, Y. E. Ihm, and N. Otsuka, *Appl. Phys. Lett.* **50**, 1364 (1987).
- ²⁰R. M. Cohen, M. J. Cherg, R. E. Benner, and G. B. Stringfellow, *J. Appl. Phys.* **57**, 4717 (1985).
- ²¹Y. Kawamura, A. Gomyo, T. Suzuki, T. Higashino, and N. Inoue, *Jpn. J. Appl. Phys., Part 2* **41**, L447 (2002).
- ²²A. G. Norman, *Spontaneous Ordering in Semiconductor Alloys*, edited by A. Mascarenhas (Kluwer, Dordrecht, 2002), Chap. 2.
- ²³Y. Zhang, A. Mascarenhas, and L. W. Wang, *Phys. Rev. B* **63**, 201312 (2001).
- ²⁴A. Gomyo, T. Suzuki, K. Kobayashi, S. Kawata, H. Hotta, and I. Hino, *NEC Res. Dev.* **35**, 134 (1994).
- ²⁵H. Cheong, A. Mascarenhas, P. Ernst, and C. Geng, *Phys. Rev. B* **56**, 1882 (1997).